OPT-*i*
An International Conference on
Engineering and Applied Sciences Optimization
M. Papadrakakis, M.G. Karlaftis, N.D. Lagaros (eds.)
Kos Island, Greece, 4-6 June 2014

MODELING OF MASONRY COMPRESSIVE FAILURE USING NEURAL NETWORKS

Vagelis Plevris and Panagiotis G. Asteris

Computational Mechanics Laboratory, Department of Civil Engineering Education,
School of Pedagogical & Technological Education
Heraklion, GR 141 21, Athens, Greece
vplevris@gmail.com, panagiotisasteris@gmail.com

Keywords: Masonry, brittle material, compressive, modeling failure criterion, failure surface, Neural Network, NN, prediction, approximation, biaxial.

Abstract. *Masonry is a material that exhibits distinct directional properties because the mortar joints act as planes of weakness. To define failure under biaxial stress, a three-dimensional surface in terms of the two normal stresses and shear stress, or the two principal stresses and their orientation to the bed joints, are required.*

Researchers have long been aware of the significance of the bed joint angle to the applied load and many experimental tests have been carried out on brick masonry discs to produce indirect tensile stresses on joints inclined at various angles to the vertical compressive load. The highest strength of masonry is observed for cases when the compressive load is perpendicular to the bed joints or in other words when the principal tensile stress at the center of the disc is parallel to the bed joints. In this case failure occurs through bricks and perpendicular joints. The lowest strength is observed when the compressive load is parallel to the bed joints or when the principal tensile stress at the center of the disc is perpendicular to the bed joints. In this case failure occurs along the interface of brick and mortar joint.

In the present study Neural Networks (NNs) are used in order to approximate the experimental failure curves of a brittle anisotropic material such as masonry. First, for each angle θ of the joints to the vertical compressive load, a Neural Network is trained with the experimental data of Page [7] as its inputs. Each one of the three NNs is asked to produce the whole 2D failure curve for each angle as its output, filling also the gaps between the experimental points with appropriate approximations. Then another bigger, "global" NN is trained which takes the results of the three NNs as inputs with the angle θ as an input, also. The new NN is then asked to fill also the gaps between the angles θ, providing the whole 3D failure surface for any angle θ. The results show the great potential of using NN for the approximation of the masonry failure under biaxial compressive stress.

1 INTRODUCTION AND METHODOLOGY

Masonry exhibits distinct directional properties due to the influence of the mortar joints. Depending upon the orientation of the joints to the stress directions, failure can occur in the joints alone or simultaneously in the joints and the blocks. The failure of masonry under uniaxial and biaxial stress state has been studied experimentally in the past by many researchers but to the authors' knowledge there have not been many attempts to apply a Neural Network (NN) for the prediction of masonry behavior in general.

Despite the fact that masonry is one of the oldest structural materials and, actually, the main element in monumental structures such as churches, castles, mosques etc., our knowledge regarding its mechanical behavior is not as thorough as it should be and many aspects of its behavior remain to be investigated. One reason for this lack of knowledge is the highly anisotropic brittle nature of masonry, which makes complicated, difficult and expensive, the realization of reliable experimental tests under conditions of biaxial stress, and, even more, under conditions of biaxial tension or heterogeneous stress. Taking into account the numerous uncertainties of the problem, a computational model, describing the masonry failure surface in a simple manner should be an efficient tool for the investigation of the behavior of masonry structures. Many analytical criteria for masonry structures have been already proposed [1][2][3][4][5][6]. Experimental investigations can also be considered as an important support to the aforementioned efforts [7][8][9][10].

Researchers have long been aware of the significance of the bed joint angle to the applied load and many experimental tests have been carried out on brick masonry discs to produce indirect tensile stresses on joints inclined at various angles to the vertical compressive load. The highest strength of masonry is observed for cases when the compressive load is perpendicular to the bed joints or in other words when the principal tensile stress at the center of the disc is parallel to the bed joints. In this case failure occurs through bricks and perpendicular joints. The lowest strength is observed when the compressive load is parallel to the bed joints or when the principal tensile stress at the center of the disc is perpendicular to the bed joints. In this case failure occurs along the interface of brick and mortar joint.

The present work utilized the experimental data reported by Page [7], referring to a total of 102 panels, which have been already used by many other researchers [2][11]. Ratios of vertical compressive stress σ_I to horizontal compressive stress σ_{II} of 1, 2, 4, 10 and ∞ (uniaxial σ_I) have been used in conjunction with a bed joint angle θ with respect to σ_I, in directions of 0°, 22.5°, 45°, 67.5° and 90°. A minimum of four tests were performed for each combination of σ_I/σ_{II} and θ.

This data set has been used in the framework of a novel methodology, which applies Neural Networks in order to approximate the experimental failure curves of a brittle anisotropic material such as masonry [12]. The aim of the study was to introduce an anisotropic (orthotropic) Neural Network – generated 3D failure surface under biaxial stress for masonry for any angle of the joints to the vertical compressive load, as described in detail in the next paragraphs. First, for each angle θ (0º, 22.5º, 45º) of the joints to the vertical compressive load, a Neural Network was trained with the experimental data of Page as inputs (3 NNs in total). Then each one of the three NNs was asked to produce the whole 2D failure curve for each angle as its output, filling also the gaps between the experimental points, thus "enriching" the experimental data with appropriate approximations. Then another bigger, “global” NN was trained using the results of the three NNs as inputs with the angle θ as an input, also. The new NN was then asked to fill also the gaps between the angles θ, providing the whole 3D failure surface for any angle θ and any ratio of σ_I/σ_{II}.

2 BIAXIAL TESTING PROCEDURE

Masonry as a composite material consisting of bricks-and-mortar joints is a multi-phase material that depicts distinct brittle and strongly anisotropic nature. This anisotropic nature makes complicated, difficult and expensive, the realization of reliable experimental tests under conditions of biaxial stress, and, even more, under conditions of biaxial tension or heterogeneous stress. In the next paragraphs, the process of both the preparation of test specimens and the tests conducted under biaxial stress state are presented in detail, with special attention to the parameters that affect the results. Furthermore, this detailed presentation will contribute to better understanding the masonry failure as well as to the better understanding of the method (simulation) since the results of the masonry failure are used as inputs to the NN model.

2.1 Preparation of Test Specimens

There are only a limited number of experiments on masonry under biaxial stress in the literature; among them are the classical experimental works of Samarasinghe [8], Page [7], and Tasios and Vachliotis [13], the findings of which have been used widely by the research community in the last 30 years for various purposes. A common characteristic of these works is that the final specimens with the correct shape and size are derived by one of the following two ways:

First way: According to Samarasinghe [8], specimens with horizontal and vertical joints (Figure 1a) are initially constructed with dimensions greater than those of the final specimens. Then a square with the desired dimensions is drawn on the surface of the wall by a pencil at the appropriate orientation to achieve the correct lay-up angle as shown in Figure 1a.

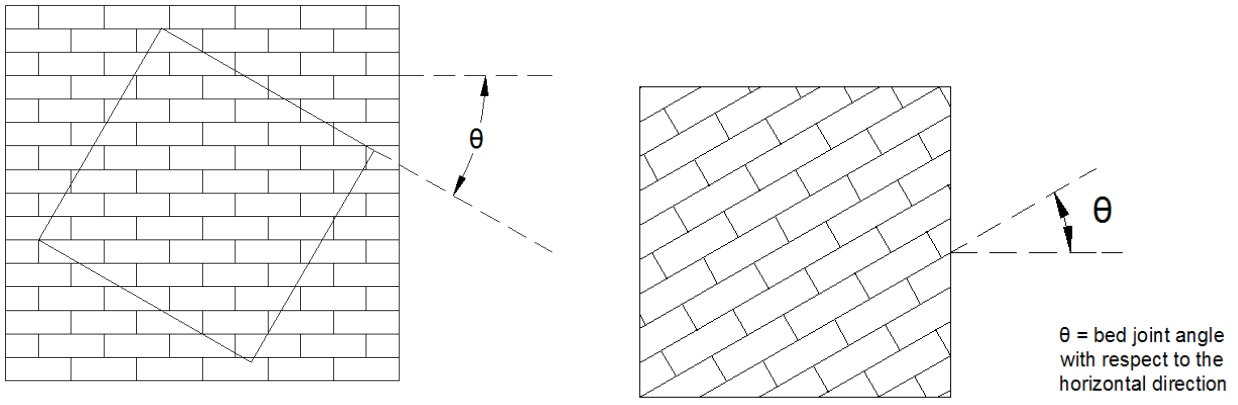

(a) (b)

Figure 1. Preparation of specimens. (a) Wall panel before saw cut, (b) Saw cut specimen.

The lay-up angle is defined as the angle between the direction of the bed joints and one of the edges of the finished test specimen. Therefore, bed joints run at oblique incidence to the edges of the finished saw-cat specimen. Five lay-up angles were selected for biaxial tests of the present study, namely 0°, 22.5°, 45°, 67.5° and 90°.

After a time-span of fourteen days the larger wall panels were cut to the required size and shape by a 'Clipper' saw (Figure 1b). Specimens in which the lay-up angle was 0° or 90°, were constructed directly without having to be derived from larger ones since they were of correct shape and size. The 'Clipper' saw has the capacity to hold impregnated diamond edge circular blades of varying thickness and diameters.

It is worth noting that circular blades of different thickness must be used on trial walls to find out the most suitable blade which gives a perfectly smooth cut without damaging the bonds of the wall. As the thickness of the blade becomes larger, more force is transmitted to the wall which causes bond failure.

Generally, two days prior to the date of testing, the 'compressive edge' of the panel (the side on which the compressive loads was going to be applied) was capped with 1:1 (cement : sand) mortar.

Second way: According to Page [7] all specimens are constructed directly to their final shape and size as follows: All brickwork is constructed horizontally on a rigid form with bricks glued to a Perspex backing sheet to ensure a constant joint thickness. Panels are made with varying bed joint angles by cutting individual bricks to the required shape before casting.

2.2 Testing rig

The biaxial testing rig is shown schematically in Figure 2. A biaxial stress state is induced in the panel by loading with hydraulic jacks in two orthogonal directions (A and B). A constant load ratio is maintained during each test by means of the spreader beam. The load in each direction is monitored by load cells immediately adjacent to the specimen.

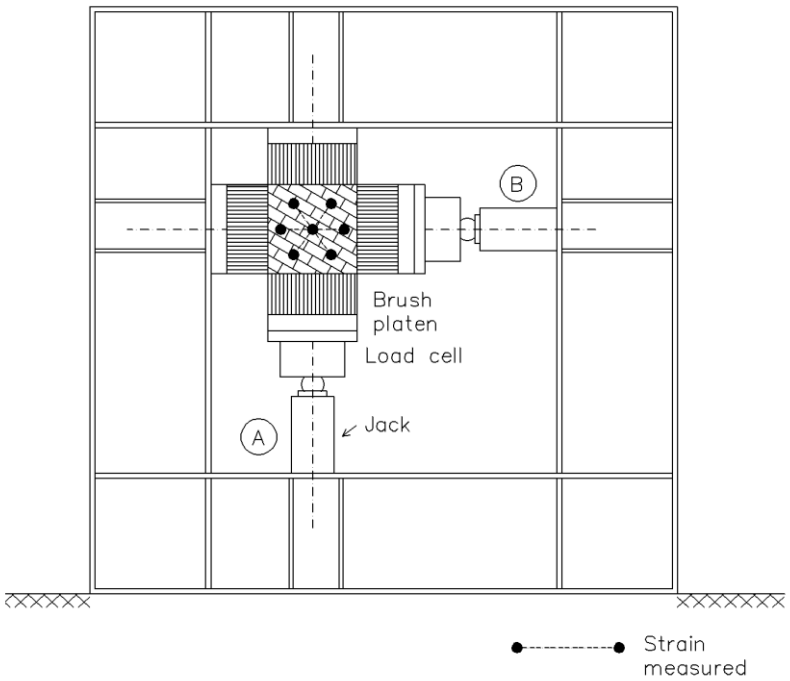

Figure 2. Biaxial testing rig.

3 BIAXIAL COMPRESSION TESTS

A total of 102 panels were tested by Page in 1981 [7]. Ratios of compressive stress σ_I to horizontal compressive stress σ_{II} of 1, 2, 4, 10 and infinity (i.e. uniaxial σ_I) were used in conjunction with bed joint angle θ with respect to the σ_I direction of 0°, 22.5°, 45°, 67.5° and 90°. Figure 3 shows the saw-cut specimens and stress directions for the three cases ϑ=0.0°, ϑ=22.5° and ϑ=45.0°. Principal stress ratios of 0 (i.e. uniaxial σ_{II}), 0.1, 0.25, 0.5 and 1 were obtained from the results using the symmetry of the panels and the loading. A minimum of four tests were performed for each combination of σ_I/σ_{II} and θ. The failure envelopes that

Page obtained by plotting mean curves for each bed joint angle are shown in Figures 4-6. These failure envelopes are based on the peak strength values obtained from running bond masonry panel tests in which a uniform loading was applied proportionally. It should be noted that in these figures, and also in all other similar figures of this paper, positive stress denotes compression.

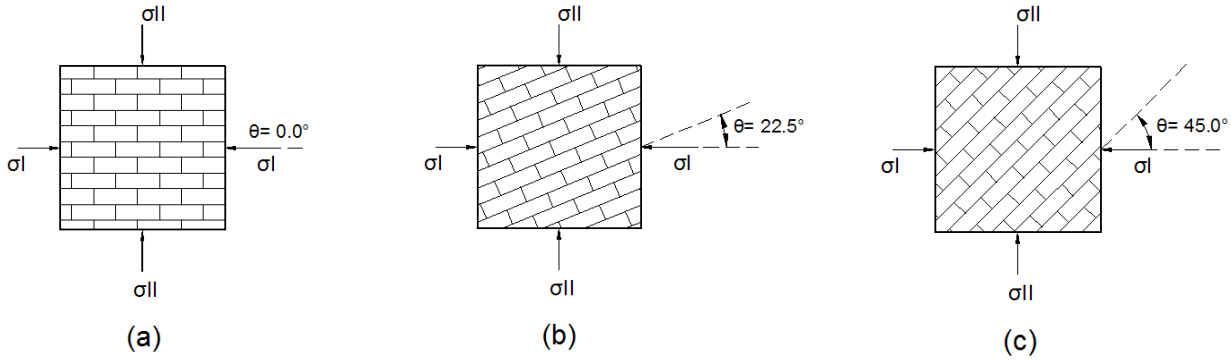

Figure 3. Saw-cut specimens and stress directions: (a) ϑ=0.0°, (b) ϑ=22.5°, (c) ϑ=45.0° [7].

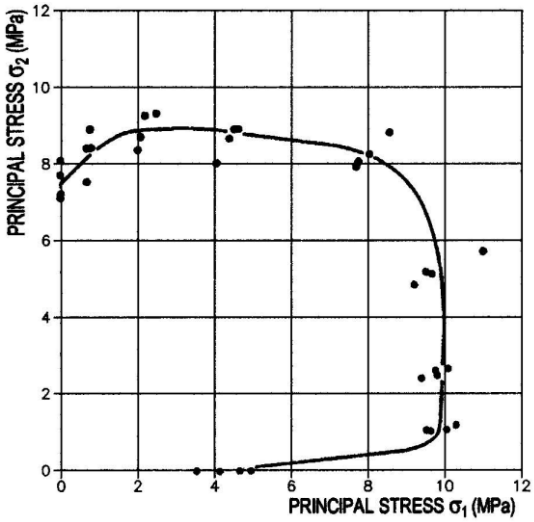

Figure 4. Failure curve of brick work under biaxial compression (ϑ=0°) [7].

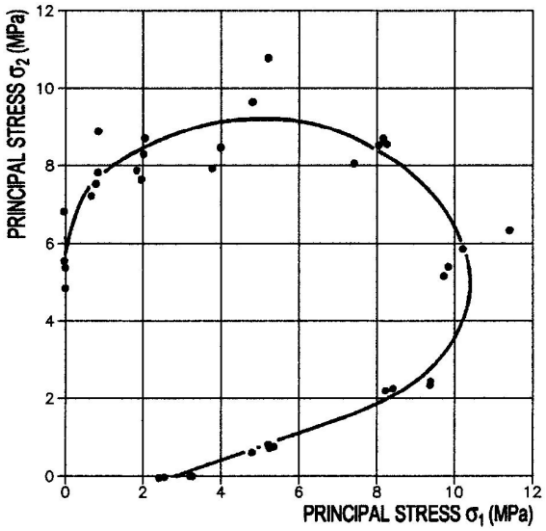

Figure 5. Failure curve of brick work under biaxial compression (ϑ=22.5°) [7].

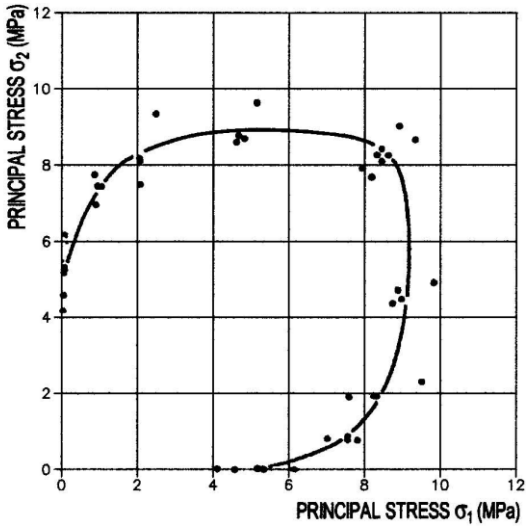

Figure 6. Failure curve of brick work under biaxial compression (ϑ=45.0°) [7].

4 ARTIFICIAL NEURAL NETWORKS

The development of artificial Neural Networks (NNs) was initially inspired and motivated by insights into how biological brains – and in particular mammalian brains – function. It was found that mammalian brains learn as connections between neurons are strengthened – the result of electrochemical processes triggered by external or internal stimuli (experiences). As in biological systems, learning involves adjustments to the synaptic connections that exist between the neurons. NNs, like human beings, learn by example.

Although parallels with biological systems are often described, there is still so little known (even at the lowest cell level) about biological systems, that the models being used for artificial neural systems seem to introduce an oversimplification of the 'biological' models. The real, biological nervous system is highly complex and includes some features that may seem superfluous based on the understanding of artificial networks.

In the first work on the processing of neural networks [14], it was shown theoretically that networks of artificial neurons could implement logical, arithmetic, and symbolic functions.

Simplified models of biological neurons were set up, now usually called perceptrons or artificial neurons. These simple models accounted for neural summation, i.e. potentials at the post-synaptic membrane would sum in the cell body. Later models also provided for excitatory and inhibitory synaptic transmission.

Artificial Neural Networks are made up of fully or partially interconnecting artificial neurons (programming constructs that mimic the properties of biological neurons). Artificial NNs may either be used to gain an understanding of biological neural networks, or for solving artificial intelligence problems without necessarily creating a model of a real biological system. *Artificial Intelligence* (AI) and *cognitive modeling* try to simulate some properties of neural networks. While similar in their techniques, AI has the aim of solving particular tasks, while cognitive modeling aims to build mathematical models of biological neural systems. In the AI field, artificial neural networks have been trained to perform complex functions in various scientific fields and have been applied successfully to identification, classification, simulation, inverse simulation, speech recognition, pattern recognition, image analysis and adaptive control, and also in order to construct software agents (in computer applications) or autonomous robots.

4.1 Neural Networks architecture

In the present study, we use *Back-Propagation Neural Networks* (BPNNs). In this type of NNs, the output values are compared with the correct answer to compute the value of a predefined error-function. By various techniques, the error is then fed back through the network. Using this information, the algorithm adjusts the weights of each connection in order to reduce the value of the error function by some small amount. After repeating this process for a sufficiently large number of training cycles, the network will usually converge to some state where the error of the calculations is small. In this case, one would say that the network has *learned* a certain target function. As the algorithm's name implies, the errors propagate backwards from the output nodes to the inner nodes. So technically speaking, back-propagation is used to calculate the gradient of the error of the network with respect to the network's modifiable weights. To adjust weights properly, one applies a general method for non-linear optimization that is called gradient descent. In order to minimize the error, the derivative of the error function with respect to the network weights is calculated, and the weights are then changed such that the error decreases (thus going downhill on the surface of the error function). For this reason, back-propagation can only be applied on networks with differentiable activation functions. Back-propagation usually allows quick convergence on satisfactory local minima for error in the kind of networks to which it is suited.

A BPNN is a feed-forward, multilayer network of standard structure, i.e. neurons are not connected in the layer but they join the layer neuron with all the neurons of previous and subsequent layers, respectively. A BPNN has a standard structure that can be written in short as

$$N - H_1 - H_2 - \ldots - H_{NL-1} - M \tag{1}$$

where N is the number of inputs, H_l is the number of neurons in the l-th hidden layer, NL is the number of layers (including the output layer) and M is the number of output neurons. Figure 7 depicts an example of a BPNN composed of an input layer with 4 neurons, two hidden layers with 3 neurons each and an output layer with 2 neurons, i.e. a 4-3-3-2 BPNN.

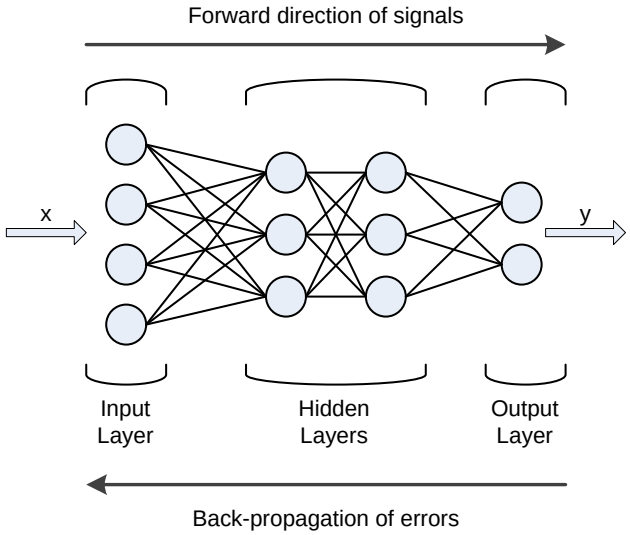

Figure 7. A three-layer 4-3-3-2 BPNN (input not counted as a layer).

4.2 Transfer functions

The choice of the transfer function may strongly influence complexity and performance of neural networks. Sigmoidal transfer functions are the most commonly used, while a large number of alternative transfer functions have been also described in the literature [15]. The transfer function used in the present study is the hyperbolic tangent function, the same for all the hidden and the input layer, while the transfer function for the output layer is a linear function. This scheme has been used in all the NNs of the present study. The output of the hyperbolic tangent function and its derivative are given by

$$a = f(n) = \tanh(n) = \frac{e^{2n} - 1}{e^{2n} + 1} = -\imath \cdot \tan(\imath n) \tag{2}$$

$$f'(n) = 4\frac{e^{2n}}{(e^{2n} + 1)^2} = 1 - a^2 \tag{3}$$

This transfer function yields output values in the interval [-1, 1], while its derivative yields output values in the interval [0, 1].

5 THREE NN MODELS (FOR EACH ANGLE Θ)

5.1 NN Architecture

We used a Back-Propagation Neural Network with two hidden layers, one input layer and one output layer for all three NNs. The input layer had one node (neuron) which corresponds to the angle φ which defines the ratio σ_{II}/σ_{I}, while the output layer had also one node which corresponds to the radius r of the point on the failure curve. These two important parameters (φ and r) will be described in detail in the following paragraphs. The two hidden layers had 8 nodes each for the first two cases (θ=0° and θ=22.5°), ending in a 1-8-8-1 BPNN architecture. For the third case (θ=45°) the two hidden layers had 12 nodes each, ending in a 1-12-12-1 BPNN architecture. These values have been chosen after some trial tests on various network architectures. The reason that the third NN requires more nodes in the hidden layer has proba-

bly to do with the number of the input data, which is different in the third case (10 points as opposed to 9 points for the first two cases, as shown in Figures 8-10.

The input and output values are normalized before the NN training and the inverse normalization is performed in order to take the NN results for other data afterwards.

5.2 Preparation of the NN Input data

The experimental data of Page [7] have been used as inputs for the first three NN models of the present study. The figures below show the original data (in a normalized form) together with the average values (as red "squares") that attempt to fit these data for each bed joint angle.

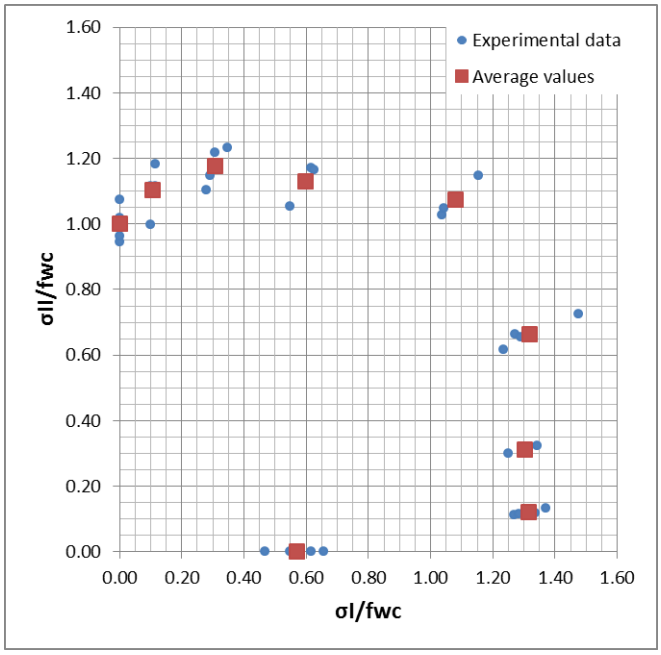

Figure 8. Normalized experimental data and average values for the θ=0° case.

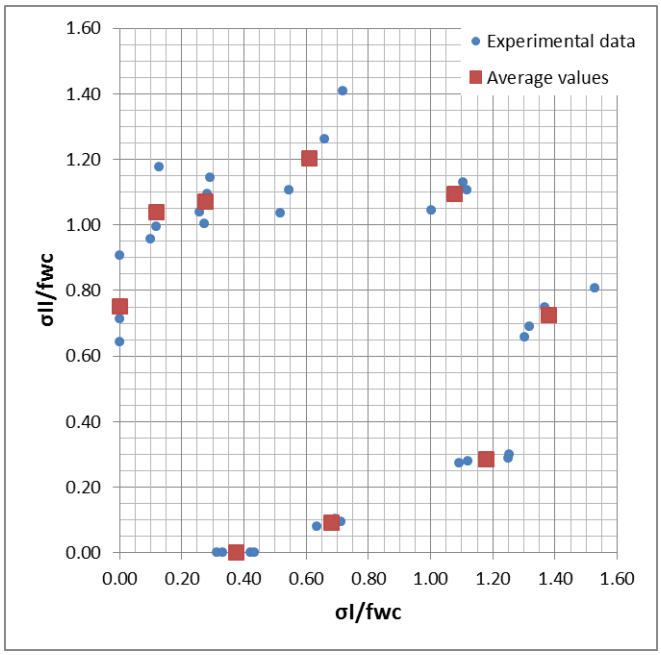

Figure 9. Normalized experimental data and average values for the θ=22.5° case.

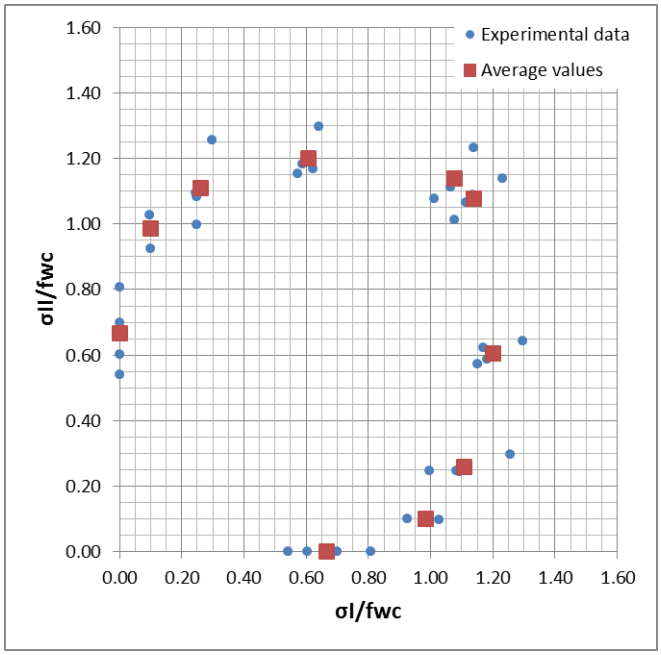

Figure 10. Normalized experimental data and average values for the θ=45° case.

It should be noted that the data for θ=45° are symmetric to the 45° line ($\sigma_I=\sigma_{II}$), due to the nature of the loading, while the cases θ=67.5° and θ=90° are "equivalent" to the cases θ=22.5° and θ=0° ("mirrored" results), respectively and should not be examined separately.

Table 1 shows the analytical data for the θ=0° case, where only the averages of σ_I/f_{wc} and σ_{II}/f_{wc} (out of four tests for each loading case) are shown, corresponding to the red "squares" points in the above figures. The quantity f_{wc} is the masonry strength for the case $\sigma_I=0$. The value of f_{wc} has been calculated as the average of the four test values as 7.56 MPa.

For the data to be suitable for the Neural Network training, a conversion to polar coordinates (r, φ) is needed, where the radius r is given by

$$r = \sqrt{\sigma_{I,aver}{}^2 + \sigma_{II,aver}{}^2} \tag{4}$$

where $\sigma_{I,aver}$ and $\sigma_{II,aver}$ are the average stresses for each loading case. The polar angle φ is given by

$$\varphi = \mathrm{Arc}\tan\left(\frac{\sigma_{II}}{\sigma_I}\right) \tag{5}$$

The polar radius r is given in the last column of the table. For each of the three angles θ (θ=0°, 22.5°, 45°), a Neural Network is trained with the angle φ as its input and the radius r as its output. Only these average values of each test (denoted as "square" points in Figures 8-10) are used as training data for the Neural Network.

Tables 2 and 3 show the corresponding data (average values) for the other two cases (θ=22.5° and θ=45°).

Average σ_I/f_{wc}	Average σ_{II}/f_{wc}	Angle φ = Atan(σ_{II}/σ_I)	Radius r
0.57	0.00	0.0000	0.5717
1.32	0.12	0.0909	1.3210
1.30	0.31	0.2353	1.3398
1.32	0.66	0.4672	1.4761
1.08	1.07	0.7820	1.5222
0.60	1.13	1.0836	1.2792
0.31	1.18	1.3156	1.2148
0.11	1.10	1.4737	1.1074
0.00	1.00	1.5708	1.0000

Table 1. Failure of Brickwork under Biaxial Compression, θ=0° [7] and relevant calculations.

Average σ_I/f_{wc}	Average σ_{II}/f_{wc}	Angle φ = Atan(σ_{II}/σ_I)	Radius r
0.38	0.00	0.0000	0.3752
0.68	0.09	0.1352	0.6890
1.18	0.29	0.2382	1.2132
1.38	0.73	0.4843	1.5581
1.08	1.09	0.7927	1.5359
0.61	1.20	1.1018	1.3493
0.28	1.07	1.3178	1.1053
0.12	1.04	1.4580	1.0467
0.00	0.75	1.5708	0.7508

Table 2. Failure of Brickwork under Biaxial Compression, θ=22.5° [7] and relevant calculations.

Average σ_I/f_{wc}	Average σ_{II}/f_{wc}	Angle φ = Atan(σ_{II}/σ_I)	Radius r
0.67	0.00	0.0000	0.6666
0.99	0.10	0.1012	0.9905
1.11	0.26	0.2301	1.1379
1.20	0.61	0.4677	1.3446
1.14	1.08	0.7565	1.5675
1.08	1.14	0.8143	1.5675
0.61	1.20	1.1031	1.3446
0.26	1.11	1.3407	1.1379
0.10	0.99	1.4696	0.9905
0.00	0.67	1.5708	0.6666

Table 3. Failure of Brickwork under Biaxial Compression, θ=45° [7] and relevant calculations.

5.3 Approximation results of the three NNs

The three NNs were trained with the input and output data of Tables 1, 2, 3 (last two columns) and then each NN was asked to produce the full curves for each bed joint angle, for a set of 100 segments (101 points). The results are shown in the figures below.

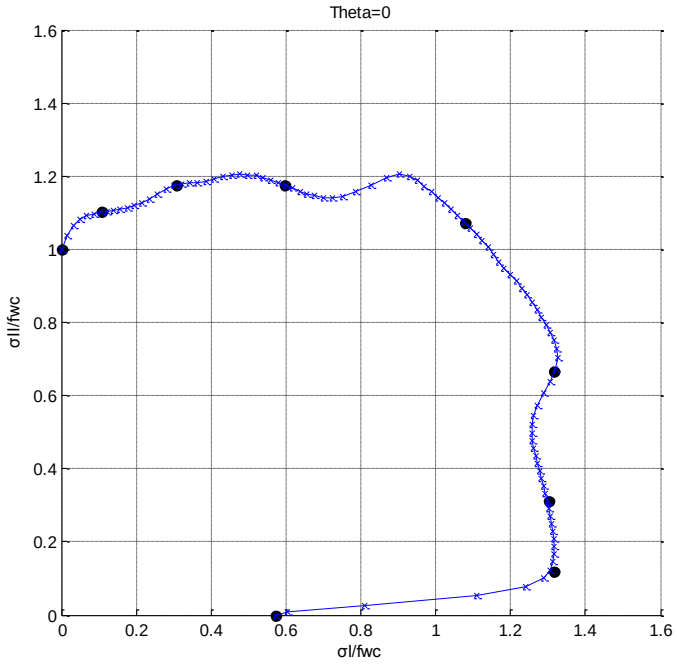

Figure 11. NN approximation result for the case θ=0°.

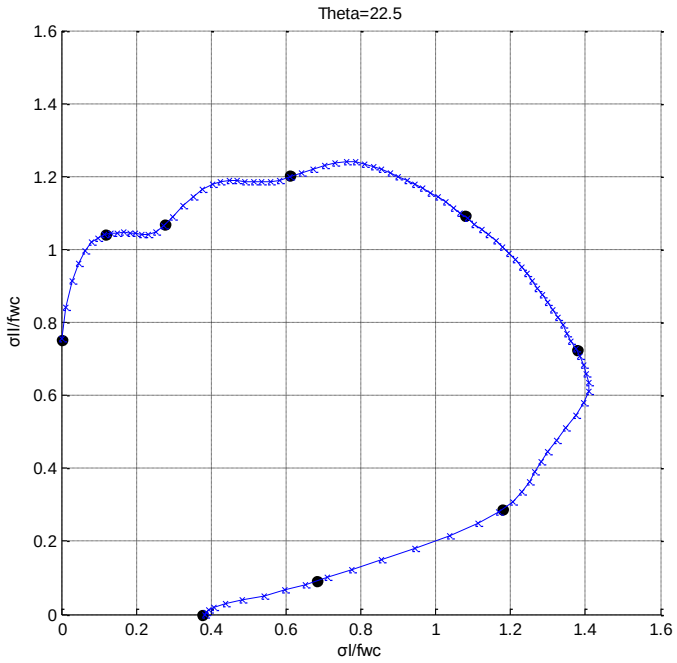

Figure 12. NN approximation result for the case θ=22.5°.

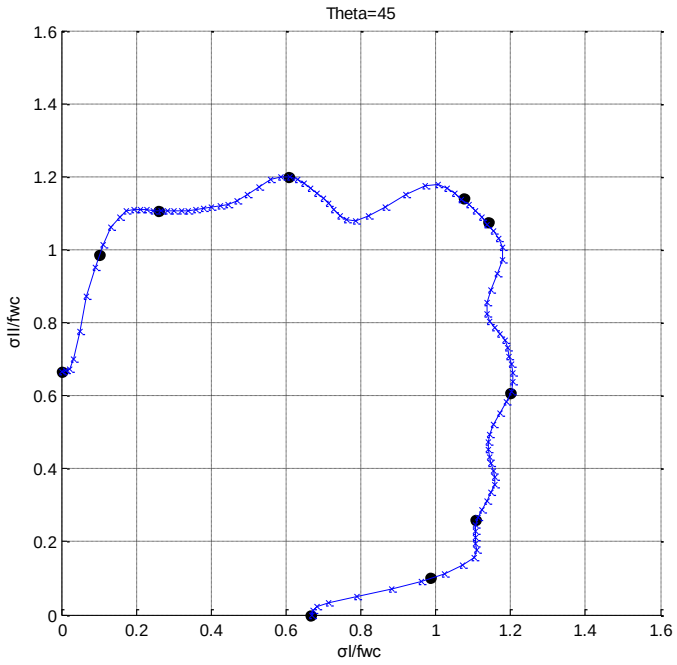

Figure 13. NN approximation result for the case θ=45°.

In the above figures, the black dots denote the input data, i.e. the data corresponding to the last two columns of Tables 1, 2, 3. The blue curve denotes the NN prediction of the fitting curve.

It can be seen that the NN managed to fit all the training data with excellent accuracy, while the approximation between the training data points appears to be adequate. An important characteristic is that for the third case (θ=45°) the NN managed to produce results that are symmetric (with good accuracy) to the line of 45° (σ_I=σ_{II}), an expected outcome due to the symmetry that masonry exhibits with respect to the 45° axis.

6 "GLOBAL" NEURAL NETWORK MODEL

In the previous part of the study, three NN Models were trained, each NN for an angle θ (0°, 22.5° and 45°). The final purpose of the study is to add also the angle θ as a parameter of the problem, thus creating a model that will be able to predict the failure curve not only for the predefined angles, but for any angle θ.

In order to achieve this, after the three NNs were trained and they had provided their results, another bigger, "Global" NN was trained which took the results of the three NNs as inputs with the angle θ as an input, also. The new NN was then asked to fill also the gaps between the angles θ, providing the whole 3D failure surface for any angle θ and any ratio of σ_{II}/σ_I.

The Global NN is also a BPNN with 9 nodes per hidden layer (2-9-9-1). The two inputs are the angles φ (0° - 90°) and θ (0° - 45°), while the output is the radius r. The transfer function of the global NN is the hyperbolic tangent function that was used also in the first three NNs. For the global NN, we use the results of the other three NNs as training patterns. This means that we have 101*3 = 303 training patterns, as we use 101 points for every angle θ (0°, 22.5° and 45°).

6.1 Global NN results

The global NN was trained and then it was asked to produce the whole 3D failure surface. The NN was asked to produce points where the angle φ was divided again in 100 segments (101 points, each segment is equivalent to 0.45°), while angle θ was divided in 64 segments (65 points, each segment is equivalent to 0.703125°). Figure 14 shows the result of the NN approximation in 3D. The red points (dots) denote the initial training set of the first three NNs, i.e. the average values gathered from the experimental results and used for the training of the initial NN.

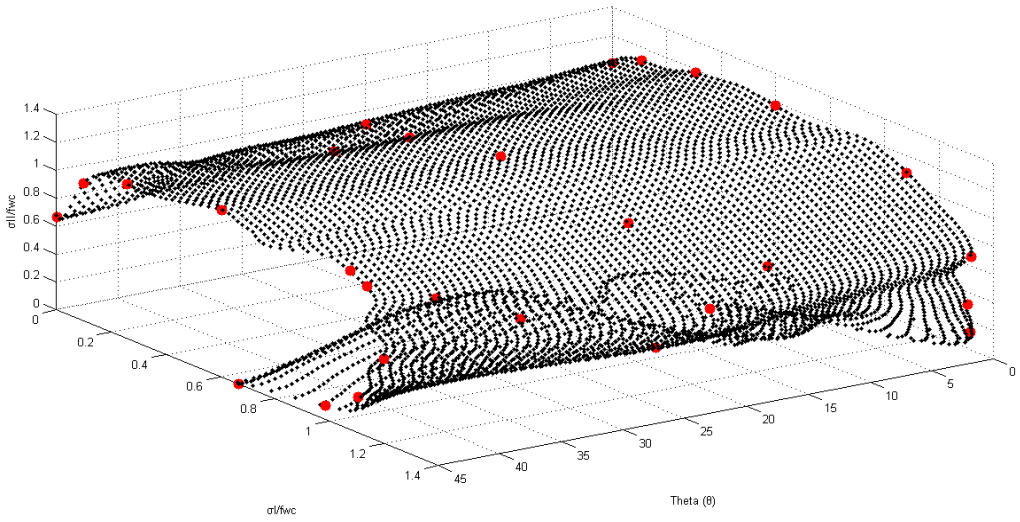

Figure 14. Global NN approximation result of the 3D failure surface (a).

Then the NN was asked to produce the 2D failure curves for five cases of angle θ (0°, 11.25°, 22.5°, 33.75° and 45°). The results are shown below, where for the three cases 0°, 22.5° and 45°) there are available experimental data (training sets of the first three NNs), that are denoted with red points (dots).

In [16], the NN-generated failure surfaces have been compared to failure surfaces generated by other well-known analytical and semi-empirical criteria, with great success.

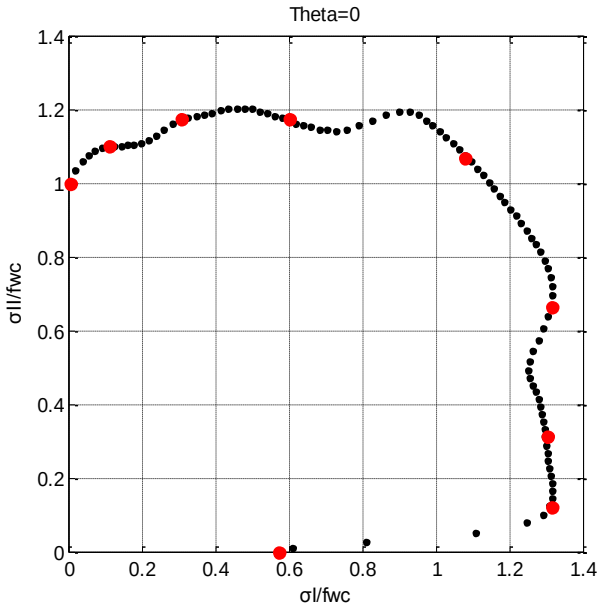

Figure 15. Global NN approximation for the θ=0° case and corresponding training points (red dots).

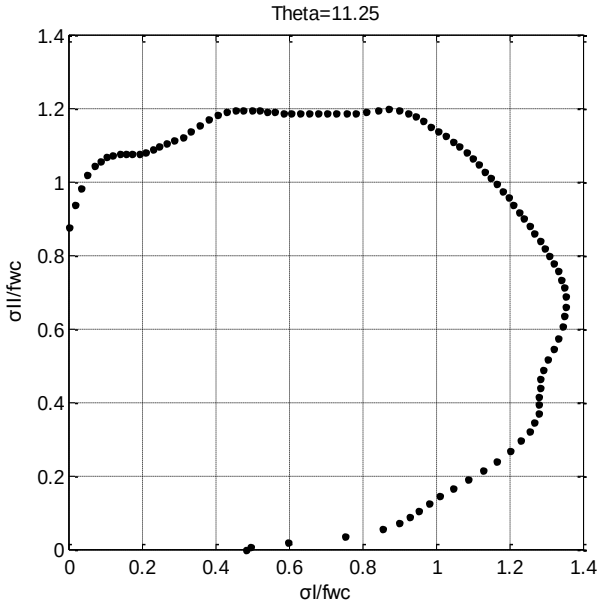

Figure 16. Global NN approximation for the θ=11.25° (no training points available).

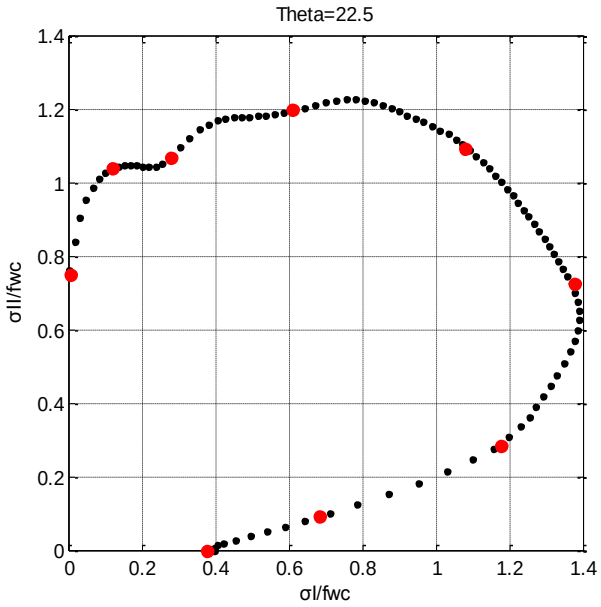

Figure 17. Global NN approximation for the θ=22.5° case and corresponding training points (red dots).

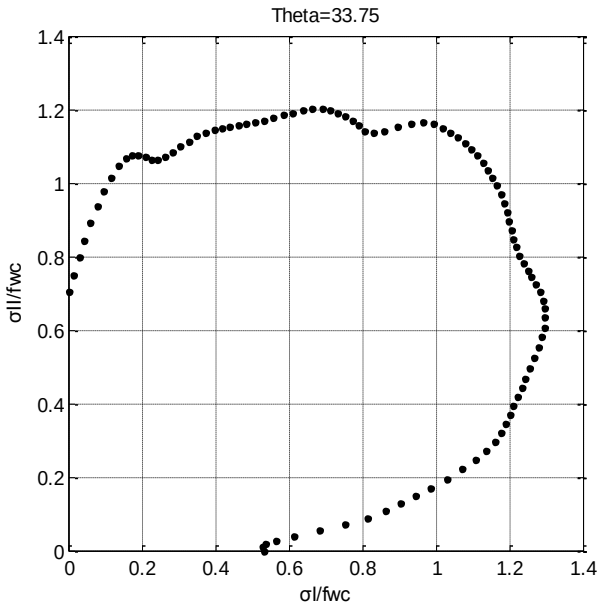

Figure 18. Global NN approximation for the θ=33.75° (no training points available)

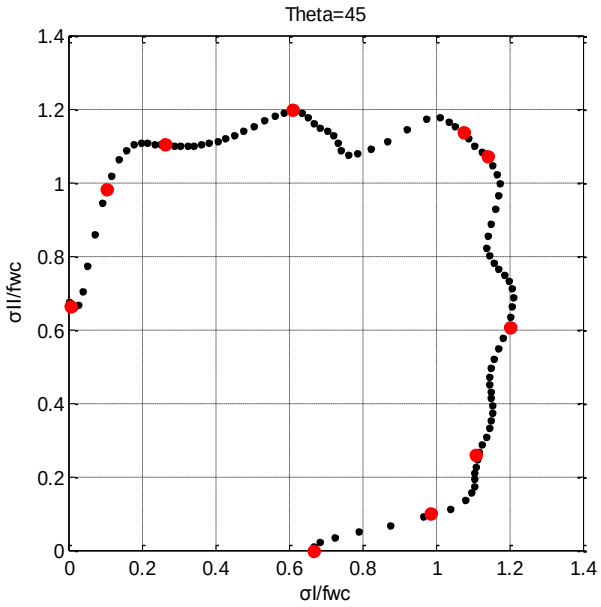

Figure 19. Global NN approximation for the θ=45° case and corresponding training points (red dots).

7 CONCLUSIONS

In the present study, results on the NN prediction of the failure of anisotropic brittle materials such as masonry are presented. In particular, Neural Networks are used in order to approximate the experimental results for masonry failure. First, for each angle θ a NN is trained with the experimental data as inputs and then each NN is asked to produce the whole failure curve for each angle as its output, filling also the gaps between the experimental points. Then, another "global" NN is trained which takes the results of the three original NNs as inputs with the angle θ as an input, also. The new NN is then asked to fill also the gaps between the angles θ, providing the whole failure 3D surface for any angle θ.

The NNs showed great performance in fitting the experimental input data, while they managed to fit all the training data with very good accuracy, also producing results that are symmetric (with good accuracy) to the line of 45° ($\sigma_I=\sigma_{II}$) for the third case (θ=45°). This is in very good agreement with the characteristic symmetry of masonry. The results show the great potential of using NN for the approximation of the masonry failure under biaxial compressive stress.

Being aware that masonry is a multi-phase material that depicts distinct brittle and anisotropic nature with wide scatter in the values of its mechanical characteristics, the following conclusions can be drawn from this investigation:

- The first three NNs managed to fit the average values of the experimental data with great accuracy. The error for the training data itself is very small, while the NN prediction for data that do not belong to the training set set appears to be also very good, providing smooth curves.
- The curves that are generated by the NNs are continuous and smooth. It should be noted that the NN curves are not necessarily convex, as most curves based on other failure criteria.

- For the case $\theta=45°$, the NN manages to provide results that are approximately symmetric to the line $\sigma_I=\sigma_{II}$.
- The "Global" NN manages to give us valuable information about angles that have not been investigated until now. The fit of the experimental data is excellent, while the NN prediction for other points appears to be also very good, providing smooth surfaces in 3D.
- The reliability of the global NN is in general high. In this paper we proposed a computational procedure for approximating failure curves in 3D, rather than giving the final results for this kind of problems. If more dense data were provided to the NN, then it could give even better results. In any case, the quality and quantity of the experimental data is very important in such problems.

REFERENCES

[1] Dhanasekar, M., Page, A. W., and Kleeman P. W., "The failure of brick masonry under biaxial stresses." Proceedings, *The Institution of Civil Engineers, Part 2, 79*, 295-313, 1985.

[2] Naraine, K., and Sinha, S., "Cyclic Behavior of Brick Masonry under Biaxial Compression." Journal of Structural Engineering, ASCE, Vol. 117, No. 5, 1336-1355, 1991.

[3] Scarpas, A., "Non-local Plasticity Softening Model for Brittle Materials / Experimental Evidence / Analytical Modelling / Preliminary Results." Research Report, Laboratory of Reinforced Concrete, National Technical University of Athens, 1991.

[4] Syrmakezis, C. A., Chronopoulos, M. P., Sophocleous, A. A., and Asteris, P. G., "Structural analysis methodology for historical buildings." Proceedings of the Fourth International Conference on Structural Studies of Historical Buildings, STREMA 95, Vol. 1, 373-382, 1995

[5] Syrmakezis, C. A., Asteris, P. G., and Sophocleous, A. A., "Earthquake resistant design of masonry tower structures." Proceedings, Fifth International Conference on Structural Studies of Historical Buildings, STREMA 97, 25-27 June, San Sebastian, Spain, 377-386, 1997

[6] Asteris, P. G., "Unified Yield Surface for the Nonlinear Analysis of Brittle Anisotropic Materials", Nonlinear Sci. Lett. A, Vol.4, No.2, 46-56, 2013.

[7] Page, A. W., "The biaxial compressive strength of brick masonry", Proc. Instn Civ. Engrs, Part 2, Vol. 71, Sept., 893-906, 1981.

[8] Samarasinghe, W., "The in-plane failure of brickwork," PhD thesis, University of Edinburgh, 1980.

[9] Page, A. W., "A biaxial failure criterion for brick masonry in the tension-tension range." The International journal of Masonry Construction, Vol. 1, No. 1, 1980.

[10] Tassios, Th. P., and Vachliotis, Ch. (1989). "Failure of masonry under heterosemous biaxial stresses." Proc. Int. Conf. Conservation of Stone, Masonry-Diagnosis, Repair and Strengthening, Athens.

[11] Syrmakezis, C.A., Asteris, P.G. (2001). Masonry Failure Criterion Under Biaxial Stress State, Journal Of Materials in Civil Engineering; American Society of Civil Engineers (ASCE), Vol. 13, Issue 1, pp. 58-64.

[12] Asteris, P.G. and Plevris, V., (2013). "Neural Network Approximation of the Masonry Failure under Biaxial Compressive Stress", 3rd South-East European Conference on Computational Mechanics (SEECCM III), Kos, Greece, 12-14 June 2013.

[13] Tassios, Th. P., and Vachliotis, Ch. (1989). ''Failure of masonry under heterosemous biaxial stresses.'' *Proc., Int. Conf. Conservation of Stone, Masonry—Diagnosis, Repair and Strengthening*, Athens.

[14] Lettvin, J. Y., Maturana, H. R., McCulloch, W. S., and Pitts, W. H. "What the Frog's Eye Tells the Frog's Brain." *Proceedings of the Institute of Radic Engineers*, 47(11), 1940-1951, 1959

[15] Fausett, L. V. (1994). Fundamentals of Neural Networks: Architectures, Algorithms, and Applications, Prentice-Hall, Inc.

[16] Plevris, V. and Asteris, P.G., (2014), "Modeling of Masonry Failure Surface under Biaxial Compressive Stress Using Neural Networks", Construction and Building Materials, 55, pp. 447-461.